Aquaculture Reports 48 (2026) 103591

Contents lists available at ScienceDirect

Aquaculture Reports

journal homepage: www.elsevier.com/locate/aqrep

Hybridization detected in a wild *Megalobrama* population via integrated biological and molecular analysis

Jie Yang, Li Zou, Siyu Fan, Min Tao, Chun Zhang, Jie Hu *, Shaojun Liu *

State Key Laboratory of Developmental Biology of Freshwater Fish, Engineering Research Center of Polyploid Fish Reproduction and Breeding of the State Education Ministry, College of Life Sciences, Hunan Normal University, Changsha 410081, China

ARTICLE INFO

Keywords:
Megalobrama
Germplasm identification
Biological traits
Microsatellite molecular markers
Hybridization

ABSTRACT

The genus *Megalobrama* is an important freshwater economic fish in China, including the *M. Amblycephala* (BSB), *M. Terminalis* (SJF), *M. Hoffmanni* (GDF), et al. In recent years, overlapping natural distributions and anthropogenic disturbances have led to increasingly severe issues of germplasm mixture and degradation within this genus. This study collected 504 samples of 11 *Megalobrama* populations from the Yangtze River, Pearl River, and other basins, and conducted multidimensional germplasm assessment. Morphological analysis revealed that three typical characteristics, body shape, swim bladder, and scale pigmentation, could accurately distinguish adult BSB, SJF, and GDF. Principal Component Analysis demonstrated significant morphological differentiation among the three species with 79.942% of cumulative contribution rate ($P < 0.05$). 7 suspected hybrid-origin individuals (BS) with intermediate characteristics between BSB and SJF were identified in a wild population from the Xiangjiang River, Hunan. Cytogenetic analysis indicated all populations were diploid (2 n = 48), but GDF exhibited a distinct karyotype (26 m+18sm+4st) compared to BSB, SJF, and BS (24 m+20sm+4st). Three species-specific microsatellite markers (TTF-3, TTF-20, TTF-32) were developed based on transcriptome sequencing, polyacrylamide gel electrophoresis, and capillary electrophoresis. BS individuals simultaneously carried 130 bp BSB-specific and 100 bp SJF-specific diagnostic markers, confirming them as hybrids. In addition, SJF demonstrated significantly higher feeding and weight gain rates than other populations, while BSB exhibited the highest condition factor ($P < 0.05$). Furthermore, SJF performed optimally with low temperature $T_{LD_{50}}$= 0.25 °C, high temperature $T_{LD_{50}}$= 32.36 °C, and hypoxia $DO_{LD_{50}}$= 0.92 mg/L. Growth and tolerance performance of self-crossing offspring from BS were intermediate between SJF and BSB. This study provides the first multi-level evidence confirming ongoing interspecific gene flow within the genus *Megalobrama*. These results represent critical data for *Megalobrama* resource conservation, selective breeding, and evolutionary research.

1. Introduction

The genus *Megalobrama*, belonging to the family Cyprinidae and subfamily Culterinae, comprises several species such as *M. amblycephala*, *M. terminalis*, *M. hoffmanni*, and *M. Pellegrini* (Chen, 1998; Luo, 1990). According to the *China Fishery Statistical Yearbook*, the annual production of bream (*Megalobrama and Parabramis*) has stabilized at approximately 770,000 tonnes over the past five years, with an annual output value exceeding 15 billion yuan (Bureau of Fisheries, 2024), underscoring their significant economic role in China's aquaculture industry.

Megalobrama are widely distributed across the basins of the Yangtze River, Yellow River, Pearl River, and Hainan Island in China. For instance, *M. amblycephala* primarily inhabits medium-sized lakes in the middle-lower Yangtze River (Pan, 1991), while *M. terminalis,* the most widely distributed species in this genus, ranges through the Yangtze, Yellow, and Amur River systems, extending to Russia's Far East (Xu and Xiong, 2008). *M. hoffmanni* occurs in the Pearl River system and Hainan Island drainage basins (Wu, 1964). Overlapping natural distributions create potential for interspecific hybridization among wild *Megalobrama* populations. Additionally, long-term artificial propagation, overfishing, and stock enhancement activities have exacerbated germplasm hybridization and degradation issues (Gao et al., 2014). Systematic collection, identification, and conservation of *Megalobrama* germplasm resources are therefore crucial for biodiversity preservation and selective breeding of improved varieties.

Fish morphological traits serve not only as fundamental criteria for

* Correspondence to: College of Life Sciences, Hunan Normal University, Changsha, Hunan 410081, China.
E-mail addresses: hujie20081402@126.com (J. Hu), lsj@hunnu.edu.cn (S. Liu).

https://doi.org/10.1016/j.aqrep.2026.103591
Received 30 September 2025; Received in revised form 24 March 2026; Accepted 8 April 2026
Available online 11 April 2026
2352-5134/© 2026 The Authors. Published by Elsevier B.V. This is an open access article under the CC BY-NC-ND license (http://creativecommons.org/licenses/by-nc-nd/4.0/).

species classification, germplasm identification, and genetic diversity studies (Chen and Wang, 2021), but also as key references for genetic breeding programs (Yan et al., 2007). Previous morphometric analyses have distinguished *Megalobrama* species (Cai et al., 2001; Song et al., 2013a). Li et al. (2002) demonstrated close phylogenetic relationships between *M. amblycephala* and *M. terminalis* using morphometrics and molecular biology (Li et al., 2002). Zeng et al. (2012) documented morphological divergence among three *M. amblycephala* populations from different basins, noting closer similarity between Liangzi Lake and Poyang Lake populations versus those from Yuni Lake (Zeng et al., 2012). Song et al. (2013) characterized morphological distinctions among all four *Megalobrama* species (Song et al., 2013b), while Chen et al. (2014) compared morphological variation across six bream populations(Chen et al., 2014). However, morphology-based identification remains limited by environmental influences and subjective interpretation.

Molecular markers provide DNA-level resolution for species discrimination. Microsatellites (Simple Sequence Repeats, SSRs), valued for stability, detectability, and short core motifs (Hamada et al., 1982), are widely employed in population genetics, germplasm assessment, genetic diversity analysis, marker-assisted selection, and evolutionary studies (Manish et al., 2020; Oliya et al., 2018; Shen et al., 2014; Singh et al., 2020; Wang et al., 2020). SSR markers have also been applied to species identification within the genus *Megalobrama*. Li et al. (2007) developed SSR primers for *M. amblycephala* via magnetic bead enrichment (Li et al., 2007b). Tang et al. (2009) generated SSR primers using 5′-anchored PCR technology(Tang et al., 2009). Gao et al. (2012) derived EST-SSR primers from *M. amblycephala* transcriptome data by Roche 454 sequencing (Gao et al., 2012). Li et al. (2014) screened species-specific SSR markers from GenBank and literature to distinguish three Culterinae species (*M. hoffmanni*, *Parabramis pekinensis*, and *Culter recurviceps*) in the Pearl River (Li et al., 2014). Unlike prior studies relying on magnetic beads or linkage maps, this study employs high-throughput transcriptome sequencing of *M. amblycephala* and *M. hoffmanni* to efficiently screen microsatellite markers, coupled with capillary electrophoresis to develop species-specific SSR markers for accurate identification of *Megalobrama* species.

Comparative analysis of biological traits, including feeding, growth, and stress tolerance, constitutes another essential approach for fish germplasm evaluation. Juvenile *Megalobrama* predominantly consume zooplankton (Pan, 1991; Xu and Xiong, 2008), but adults exhibit distinct dietary preferences. *M. amblycephala* feeds mainly on aquatic plants like *Hydrilla verticillata* (Wang et al., 2019). *M. terminalis* consumes bivalves (e.g., *Limnoperna lacustris*), shrimp, and aquatic vegetation (Feng, 2009). *M. hoffmanni* favors animal matter, primarily mollusks such as *Corbicula fluminea*, supplemented by higher aquatic plants (Xu and Xiong, 2008). *M. pellegrini* selects aquatic vascular plants and animal-based foods (Li et al., 2007a). Growth rates of *Megalobrama* typically peak during years 2–3 after rapid initial growth, declining from year 3 onward (Wu, 1964). Comparative studies of feeding and growth traits facilitate core germplasm screening and parental selection. Environmental tolerance in fish refers to their survival capacity and adaptability under various stressors, including hypoxia (Gong et al., 2020), thermal extremes (Blödorn et al., 2021; Kraitavin et al., 2019), saline-alkaline exposure (Takata et al., 2021), and ammonia toxicity (Pan et al., 2023). Water temperature and dissolved oxygen are universally recognized as pivotal environmental factors influencing aquatic organisms' physiology and behavior (Hu et al., 2024). Stress resilience in fish serves as the primary criterion for identifying superior germplasm and constitutes a central objective in guiding selective breeding programs.

This study collected founder stocks, cultured populations, and wild populations of three *Megalobrama* species, *M. amblycephala*, *M. terminalis*, and *M. hoffmanni*, from diverse water systems. By integrating multi-level comparative assessments of morphology, cytogenetics, microsatellite molecular markers, growth performance, and environmental tolerance, this study revealed interspecific differences in growth performance and environmental adaptability. Notably, hybrid individuals were identified within a wild *Megalobrama* population. This research provides fundamental data for germplasm identification, resource conservation, and genetic improvement in *Megalobrama*, ultimately advancing sustainable development in aquaculture.

2. Materials and methods

2.1. Experimental fish

From 2023–2025, this study collected 504 specimens representing 11 populations of founder stocks, cultured stocks, and wild populations of *M. amblycephala* (abbreviated as BSB), *M. terminalis* (SJF), and *M. hoffmanni* (GDF) from diverse aquatic systems across China (Table A1). The sampling comprised 180 BSB specimens from 4 populations, 163 SJF specimens from 4 populations, and 161 GDF specimens from 3 populations (Table A1). Detailed sampling locations were listed in Table A1. All live samples collected were implanted with PIT tags and utilized for mophological, cytogenetic and molecular studies.

2.2. Self-crossing of the Megalobrama species

For subsequent comparison of growth performance and environmental tolerance, 9 sexually mature individuals (3 females and 6 males) from each wild population of BSB, SJF and GDF, as well as 7 suspected interspecific hybrid individuals (3 females and 4 males) from the wild population of BSB, were used for artificial breeding to produce self-crossing offspring in 2024. The mature eggs were fertilized with the mature sperm and the embryos were hatchling in freshwater at 22–24 °C, according to the protocol in our previous study by Hu et al. (2012). All the *Megalobrama* fish were maintained at the "Engineering Research Center of Polyploid Fish Reproduction and Breeding of the State Education Ministry", School of Life Sciences, Hunan Normal University. The experimental protocols were approved by the Ethics Committee of Hunan Normal University.

2.3. Measurement of morphological traits

The morphometric measurements in this study followed the standardized protocols established by Hubbs and Lagler (C.L. and K.F., 1964). For morphometric analysis, adult fish from all the BSB, SJF, and GDF populations were anesthetized using MS-222 (200 mg/L) for 5 min. Meristic traits including counts of dorsal fin rays, pectoral fin rays, pelvic fin rays, anal fin rays, and lateral line scales were recorded, followed by body mass measurement and photographic documentation. Photographs were processed using ImageJ-win64 software. Standardization procedures were applied to eliminate size-dependent variation based on eight normalized morphometric ratios: total length/body length (L_T/L_S), body depth/body length (D_B/L_S), head length/body length (L_H/L_S), caudal peduncle length/body length (L_{CP}/L_S), snout length/head length (L_M/L_H), eye diameter/head length (D_E/L_H), caudal peduncle length/caudal peduncle depth (L_{CP}/D_{CP}), and caudal fin length/caudal peduncle length (L_C/L_{CP}). Principal Component Analysis (PCA) of the eight morphological indices from 36, 18, 18 individuals of BSB, SJF, and GDF wild population was performed to evaluate interspecific morphological similarities and divergences within *Megalobrama* populations.

2.4. Preparation of chromosome and measurement of DNA content

The experimental methodology was adapted from "Distant Hybridization in Fish" (Liu, 2015). DNA content was quantified using flow cytometry (CytoFLEX, Beckman) according to the protocol of CyStain PI Absolute T kit, with mean DNA values determined from caudal fin samples of all the 504 experimental fish across populations. Additionally, chromosome preparations were obtained through short-term

peripheral blood lymphocyte culture of three specimens per population. 0.2–0.3 mL peripheral blood samples were collected from the caudal vasculature, using syringes pre-coated with 0.2 mL of 0.1% heparin sodium solution. Chromosome number and morphology with subsequent karyotype analysis were documented using a Leica DM2500 microscope. Good quality metaphase spreads were used for analysis of karyotype and chromosomes were classified by referring to previous standards (Hu et al., 2012; Liu, 2015).

2.5. Identification of microsatellite molecular markers

Transcriptome data of *M. amblycephala* and *M. hoffmanni* were obtained using high-throughput sequencing on the Illumina NovaSeq 6000 platform. SSR detection in Unigenes was performed with MISA software (http://pgrc.ipk-gatersleben.de/misa/) (Fig. A1). 77 SSR primer pairs were designed (Tables A2, A3) and synthesized by Sangon Biotech (Shanghai, China). 0.5 cm of fin clips were collected from specimens after anesthesia with MS-222 (200 mg/L, 5 min) and individual labeling. Genomic DNA from all the populations was extracted using the Marine Animal Tissue DNA Extraction Kit (Tiangen Biotech, China), with quality and concentration assessed by 2.2% agarose gel electrophoresis and multi-mode microplate reader. The PCR reactions were performed in a final volume of 50 μL according to the protocol of premix Taq (Takara), with the cycling conditions: (i) 95 ℃ for 5 min; (ii) 34 cycles of 95 ℃ for 30 s, Tm for 40 s, and 72 ℃ for 1 min; and (iii) 72 ℃ for 10 min. Following preliminary screening via PCR amplification and polyacrylamide gel electrophoresis (PAGE), precise allele size was determined through capillary electrophoresis (CE) using the Qsep100 Bio-Fragment Analyzers.

To ensure the reliability of the selected microsatellite loci for species identification, the potential presence of null alleles was tested. The analysis was performed using the software Micro-Checker v2.2.3, which employs methods based on homozygote excess and allele frequency distributions to detect genotyping errors due to null alleles. The analysis was conducted with a confidence interval of 95% and 1000 randomizations.

2.6. Feeding and growth performance analysis

For the growth and tolerance trials, 120 healthy self-crossing offspring with comparable size were selected from each *Megalobrama* species, with initial mean weights and lengths as follows: for BSB, 42.6 ± 0.46 g and 10.1 ± 0.16 cm; for SJF: 37.29 ± 0.80 g and 9.46 ± 0.40 cm; for GDF, 43.99 ± 1.17 g and 11.37 ± 0.12 cm; for suspected hybrids, 41.0 ± 0.73 g and 9.2 ± 0.08 cm. Fish were stocked at 25 kg/m^3 density in separate tanks within a recirculating aquaculture system (RAS). Fish were fed twice daily at approximately 09:00 and 17:00, and continuous oxygenation was provided via air diffusers.

Six months of feeding trials were conducted using commercial feed with 37% crude protein, 6% crude lipid, 25–40% starch, 6% crude fiber (Tongwei Co., Ltd.), and duckweed (*Wolffia globosa*) with 22.7–35% protein, 4.0–5.8% fat, and 20–40% starch, 9.8– 16.5% crude fiber (Thongthung et al., 2024; Seephua et al., 2025). Water temperature and feed intake were continuously monitored. This study compared duckweed consumption rates among 30 individuals of different species under two thermal regimes of 19.4 ± 2.3 °C and 14.1 ± 1.9 °C. Commercial feed trials were conducted under 20.8 ± 2.9 °C and 13.1 ± 2.4 °C, respectively. Growth performance metrics were calculated as follows:

Daily Feed Intake (DFI, g) = $F_1 + F_2$

Daily Feeding Rate (DFR, %) = (DFI / W) × 100

Weight Gain Rate (WGR, %) = [(W_2 - W_1) / W_1] × 100

Specific Growth Rate (SGR, %/day) = [(ln W_2 - ln W_1) / t] × 100

Condition Factor (CF, g/cm^3) = (W / L_S ^{3}) × 100

Of which:
W_1 = Initial mean body weight (g)
W_2 = Final mean body weight (g)
W = Mean body weight during trial (g)
L_S = Standard length (cm)
F_1, F_2 = Morning/evening feed consumption (g)
t = Trial duration (days)

2.7. Low temperature and high temperature tolerance trials

Following the feeding trials, thermal tolerance assessments were conducted on the *Megalobrama* fish. For the cold stress experiment, 30 individuals from each species were fasted for 24 h. Water temperature was reduced from 9.9 ± 0.2 °C at 0.1 °C/min using a refrigeration unit (Aoling Hengye, China), recording behavioral responses at each temperature interval, temperature at loss of equilibrium (LT_{LOE}), temperature at overturning (LT_{OT}), low-temperature median lethal dosage ($LT_{LD_{50}}$), and cumulative mortality. Throughout the cooling phase, aeration was maintained via air diffusers without water exchange until 100% mortality occurred. For the high-temperature stress test, fish (n = 30 from each species) were similarly fasted for 24 h prior to experimentation. Water temperature was elevated from 22.3 ± 0.5 °C at a constant rate of 0.1 °C/min using immersion heaters, with continuous monitoring of real-time behavioral status, the HT_{LOE}, HT_{OT} and $HT_{LD_{50}}$ temperatures, and cumulative mortality.

2.8. Hypoxia tolerance trials

Following a 24-hour fasting period, the experimental fish (n = 30 from each species) underwent standardized hypoxia tolerance assessment. DO concentrations were regulated through blending of nitrogen and oxygen gases , and continuously measured and recorded using a portable water quality meter (Smart Sensor AR8406, China). The initial dissolved oxygen (DO) level in water was maintained at 8.1 ± 0.5 mg/L. The DO was reduced to 4.0 mg/L within 60 min and maintained for 30 min, then further decreased to 2.0 mg/L within 30 min with another 30-minute maintenance period. Subsequently, graded concentrations from 1.8 to 0.9 mg/L were implemented in 0.1 mg/L decrements. The following parameters were recorded: DO values at loss of equilibrium (DO_{LOE}), at overturning (DO_{OT}), median lethal dosage ($DO_{LD_{50}}$).

2.9. Data analysis

For the comparison of morphological and physiological factors of different species, all data were presented as mean ± standard error (mean ± SE). Normality was evaluated using the Shapiro-Wilk test before the statistical significance of differences was determined. If the test of normality were violated, the Kruskal-Wallis H test was applied to conduct the nonparametric test. If the test of normality were not violated, the data were analyzed by a one-way ANOVA with $p < 0.05$ in IBM SPSS Statistics 26 (IBM, Armonk, NY, USA).

3. Results

3.1. Morphological analysis

3.1.1. Morphological characters

Morphological characters of the *Megalobrama* fish were presented in Fig. 1. Significant interspecific variations in scale patterning were observed. BSB exhibits bluish-gray coloration (Fig. 1A) with scales featuring grayish-white bases and dark gray margins, accompanied by longitudinally aligned black striations (Fig. 1B). SJF displays grayish-black pigmentation (Fig. 1E), and was characterized by centrally lightened scales bordered by dark edges (Fig. 1F). Whereas GDF shows

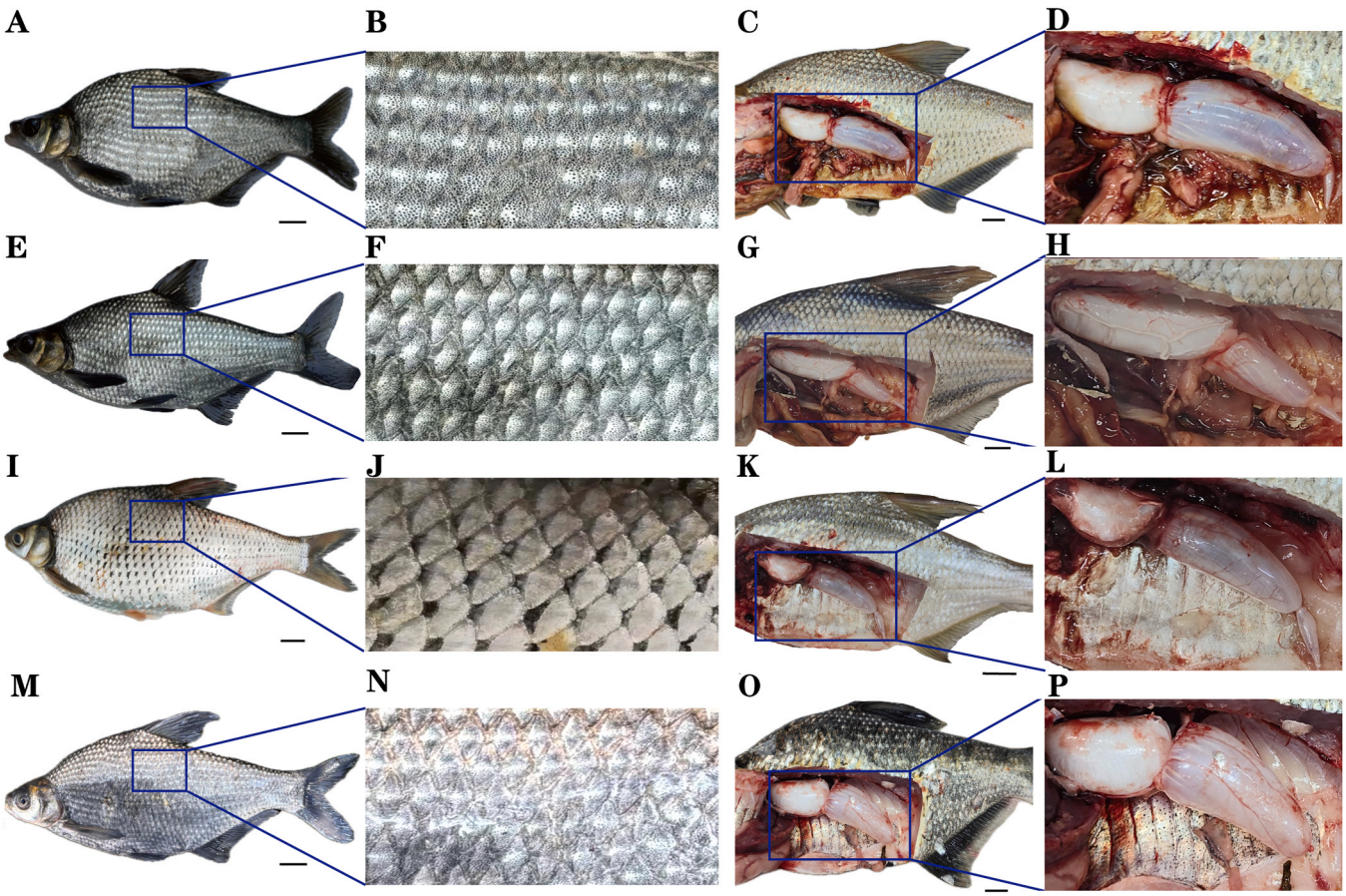


Fig. 1. The appearance, surface scales and swim bladder of the *Megalobrama* fish. A: Outline drawing of BSB. B: Scale diagram of BSB. C: Swim bladder diagram of BSB. D: Enlarged view of the swim bladder of BSB. E: Outline drawing of SJF. F: Scale diagram of SJF. G: Swim bladder diagram of SJF. H: Enlarged view of the swim bladder of SJF. I: Outline drawing of GDF. J: Scale diagram of GDF. K: Swim bladder diagram of GDF. L: Enlarged view of the swim bladder of GDF. I: Outline drawing of BS. J: Scale diagram of BS. K: Swim bladder diagram of BS. L: Enlarged view of the swim bladder of BS. Bar = 1 cm.

silvery-white body color (Fig. 1I), with distinctive dark basal spots on lateral scales (Fig. 1J). All examined *Megalobrama* populations possessed tripartite swim bladders comprising anterior, middle, and posterior chambers, with the posterior chamber being the smallest. Differential length ratios between middle and anterior chambers were recorded (Table 1). Both BSB and GDF demonstrated larger middle chambers relative to anterior chambers (Fig. 1C, D, K, L), with middle/anterior chamber ratios of 1.52 ± 0.14 and 1.20 ± 0.10, respectively. Conversely, SJF exhibited larger anterior chambers (Fig. 1G, H), yielding a middle/anterior ratio of 0.76 ± 0.10.

BSB displayed significantly greater body depth relative to body length (0.41 ± 0.02) compared to SJF (0.34 ± 0.02) and GDF (0.34 ± 0.02) ($P < 0.05$), indicating a dorsally compressed body form. GDF exhibited a significantly greater caudal peduncle length-to-depth ratio (1.10 ± 0.09) compared to SJF (0.91 ± 0.07) and BSB (0.77 ± 0.03) ($P < 0.05$), indicating an elongated caudal peduncle morphology (Table 2). Meristic counts showed no significant interspecific differences (Table 3) ($P > 0.05$).

Notably, seven morphologically distinct individuals, which diverged from the three described species (Fig. 1M), were identified within the BSB wild population collected from the Xiangjiang River (Yueliangwan section, Hunan, China). These individuals exhibited intermediate morphology between *M. amblycephala* and *M. terminalis*. Their lateral scales lack distinct white spotting, displaying faintly pigmented central regions with dark gray margins (Fig. 1N). The swim bladder morphology aligns with BSB and GDF, featuring a middle chamber exceeding the anterior chamber (Fig. 1O,P), with a middle/anterior chamber length ratio of 1.32 ± 0.15 intermediate between BSB (1.52 ± 0.14) and SJF (0.76 ± 0.10) (Table 1). Furthermore, their eight morphometric indices positioned intermediately between BSB and SJF, marginally closer to SJF (Table 2). Based on these diagnostic characteristics, these individuals were preliminarily classified as putative hybrids, hereafter designated as "BS".

Table 1
Statistics of swim bladder length of the *Megalobrama* fish.

Species	BSB	SJF	GDF	BS
Middle chamber head/front chamber head	1.52 ± 0.14	0.76 ± 0.10	1.20 ± 0.10	1.32 ± 0.15

Table 2
Measurable characters of the *Megalobrama* fish.

Species	BSB	SJF	GDF	BS
L_T/L_S	1.21 ± 0.02	1.28 ± 0.02	1.23 ± 0.02	1.26 ± 0.02
D_B/L_S	0.41 ± 0.02^a	0.34 ± 0.02^b	0.34 ± 0.01^b	0.37 ± 0.01^a
L_H/L_S	0.23 ± 0.02	0.26 ± 0.02	0.25 ± 0.01	0.26 ± 0.02
L_{CP}/L_S	0.10 ± 0.01	0.09 ± 0.01	0.11 ± 0.01	0.10 ± 0.01
L_M/L_H	0.17 ± 0.02	0.23 ± 0.02	0.21 ± 0.02	0.22 ± 0.02
D_E/L_H	0.28 ± 0.03	0.34 ± 0.03	0.37 ± 0.02	0.33 ± 0.02
L_{CP}/D_{CP}	0.77 ± 0.03^a	0.91 ± 0.07^{ab}	1.10 ± 0.09^b	0.82 ± 0.06^a
L_C/L_{CP}	2.13 ± 0.07^c	3.12 ± 0.41^a	2.30 ± 0.30^c	2.52 ± 0.10^b

^{a}, ^{b} and ^{c} represent the significant difference ($P < 0.05$).

Table 3
Countable characters of the *Megalobrama* fish.

Species	BSB	SJF	GDF	BS
Lateral line	54.9 ± 1.9 (53–57)	54.7 ± 1.2 (53–56)	53.8 ± 1.1 (52–55)	52.4 ± 1.4 (51–54)
Above lateral line	11.4 ± 0.7 (10–12)	11.3 ± 0.7 (10–12)	10.1 ± 0.8 (9–11)	10.8 ± 0.7 (10–12)
Under lateral line	8.5 ± 0.5 (8–9)	8.3 ± 0.7 (7–9)	7	8.4 ± 0.8 (7–10)
Dorsal fin	III+ 7	III+ 7	III+ 7	III+ 7
Pectoral fin	I+ 15.9 ± 0.7 (I+15–17)	I+ 14.3 ± 0.9 (I+13–16)	I+ 14.8 ± 0.7 (I+14–16)	I+ 15.6 ± 0.5 (I+15–17)
Pelvic fin	I+ 8	I+ 8	I+ 8	I+ 8
Anal fin	III+ 26.1 ± 1.1 (III+25–28)	III+ 24.9 ± 1.1 (III+23–26)	III+ 24.4 ± 0.7 (III+23–26)	III+ 24.8 ± 0.7 (III+24–26)

3.1.2. Principal component analysis (PCA)

PCA based on eight morphological indices revealed that the first three principal components (PCs) accounted for 45.475%, 22.109%, and 12.358%, respectively, with a cumulative contribution rate of 79.942%, which could essentially reflect the information contained in the comprehensive metrics (Table A4). PC1 was predominantly influenced by the body shape characteristics such as D_B/L_S, D_E/L_H, and L_{CP}/D_{CP}. PC2 was primarily driven by the head characteristics including L_T/L_S, L_H/L_S, and L_M/L_H. PC3 was mainly associated with caudal features such as L_{CP}/L_S and L_C/L_{CP}.

According to the PCA scatter plot (Fig. 2), along PC1, BSB clustered on one side with minimal overlap with SJF, GDF, and BS populations, while SJF and GDF partially overlapped and were difficult to distinguish. BSB' s significantly greater body depth drives separation on body shape-related PC1. Along PC2, all *Megalobrama* fish showed overlapping distributions, though SJF and GDF displayed limited non-overlapping regions, suggesting relatively larger cephalic divergence between these two species. Along PC3, a minority of GDF clusters showed separation from other groups, indicating that *M. hoffmanni* possesses characteristically elongated caudal peduncles. Across all three principal components, BS individuals consistently overlapped with both BSB and SJF clusters, demonstrating morphological intermediacy consistent with their suspected hybrid origin.

3.2. DNA content and chromosome spreads

DNA content analysis, particularly the comparative profiles of BSB (Fig. 3A), SJF (Fig. 3D), GDF (Fig. 3G), and BS (Fig. 3J), is presented in Fig. 3. Flow cytometric analysis revealed no significant differences in DNA content among BSB, SJF, GDF, and BS ($P > 0.05$). Chromosomal preparations from peripheral blood lymphocytes confirmed consistent diploidy ($2n = 48$) across all the populations. karyotype analysis demonstrated: BSB with 24 metacentric (m) + 20 submetacentric (sm) + 4 subtelocentric (st) chromosomes (Fig. 3B-C), SJF exhibiting 24 m+ 20sm+ 4st (Fig. 3E-F), and GDF displaying 26 m+ 18sm+ 4st (Fig. 3H-I). All karyotypes were dominated by metacentric and submetacentric chromosomes. Notably, BSB and SJF shared identical karyotype configurations, whereas GDF possessed one additional metacentric pair and one fewer submetacentric pair. The hybrid BS population displayed cytogenetic characteristics indistinguishable from BSB and SJF, evidenced by non-significant DNA content variation ($P > 0.05$) and an identical karyotype of 24 m+ 20sm+ 4st (Fig. 3K-L).

3.3. Identification and analysis of microsatellite in PAGE

High-throughput transcriptome sequencing enabled the screening of 77 pairs of microsatellite primers, with 60 pairs (78% amplification success rate) demonstrating fragment amplification across BSB, SJF, and GDF populations by PAGE. 13 primers, BF-4, BF-5, BF-6, BF-7, BF-24, BF-29, BF-31, TTF-3, TTF-8, TTF-10, TTF-20, TTF-23, TTF-32, exhibited high interspecific compatibility and robust polymorphism. Notably, three specific primers, TTF-3, TTF-20, and TTF-32, generated diagnostic fragments distinguishing each species (Fig. 4). In addition, the null allele test using Micro-Checker indicated no significant evidence of null alleles at any of the three loci across all sampled individuals ($p > 0.05$). TTF-3 amplified a 130 bp BSB-specific band (Fig. 4A), TTF-20 produced a 125 bp GDF-specific band (Fig. 4B), and TTF-32 yielded a 100 bp SJF-specific band (Fig. 4C), providing unambiguous species identification.

In the morphologically distinct BS individuals from wild BSB populations, which displayed swim bladder feature resembling BSB but external morphology closer to SJF, molecular analysis revealed co-amplification of both parental markers: the 130 bp BSB-specific fragment with TTF-3 (Fig. 4D) and the 100 bp SJF-specific fragment with TTF-32 (Fig. 4E). This dual-evidence confirms their hybrid origin from the hybridization event between *M. amblycephala* and *M. terminalis*.

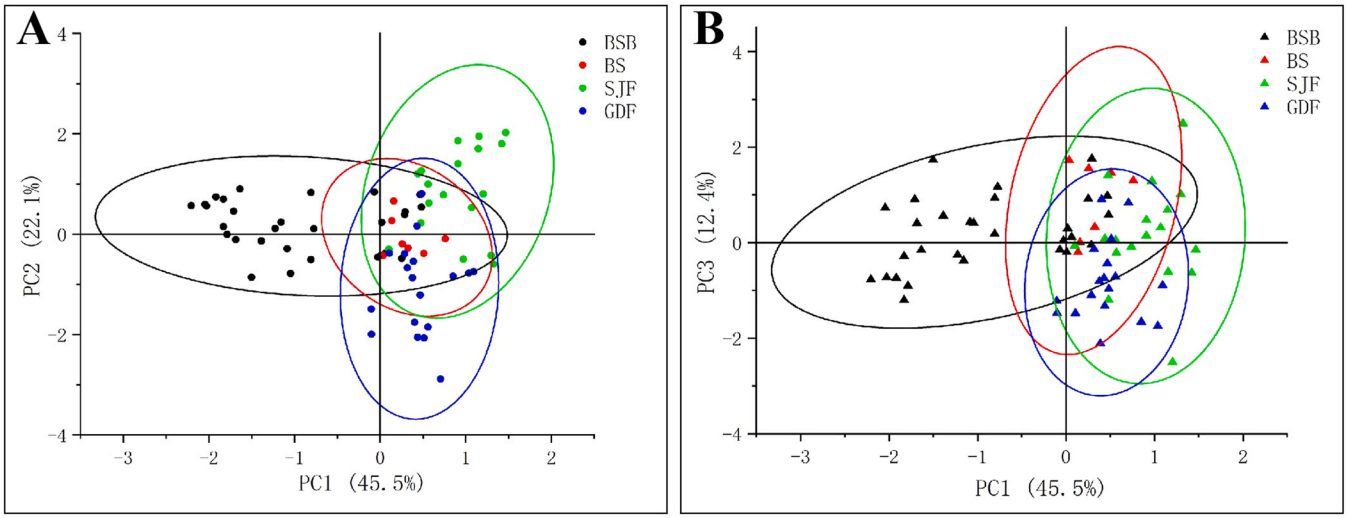


Fig. 2. PCA scatter plots of the *Megalobram* fish. A: The first and second main components. B: The first and third main components.

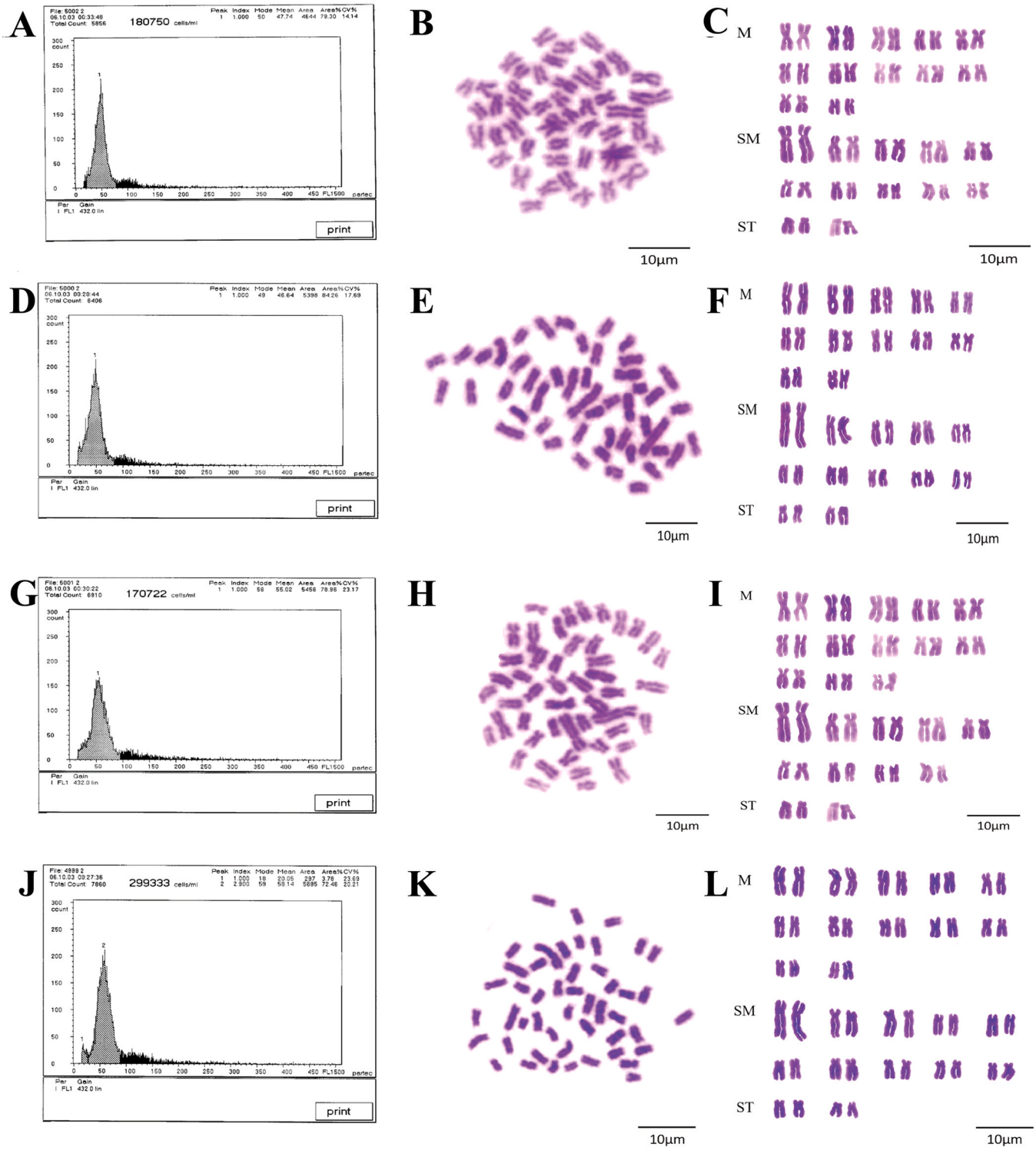
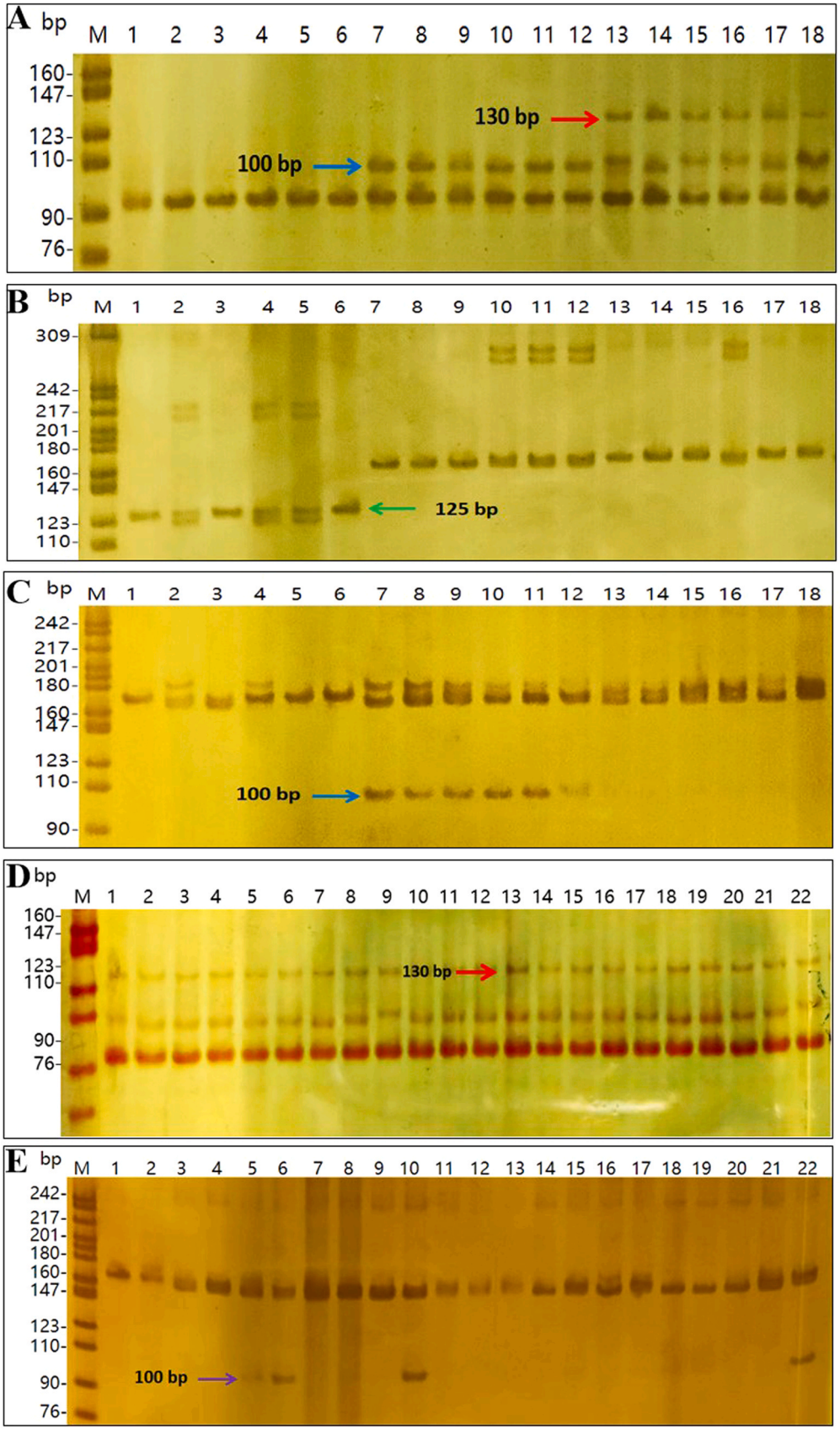


Fig. 3. DNA content and chromosome spreads of the *Megalobrama* fish. A: The mean DNA content of BSB (peak1 : 47.74). B: Chromosome speads of BSB, 2 n = 48. C: The karyotype of BSB, 24 m+ 20sm+ 4st. D: The mean DNA content of SJF (peak1 : 46.64). E: Chromosome speads of SJF, 2 n = 48. F: The karyotype of SJF, 24 m+ 20sm+ 4st. G: The mean DNA content of GDF (peak1 : 55.02). H: Chromosome speads of GDF, 2 n = 48. I: The karyotype of GDF, 26 m+ 18sm+ 4st. J: The mean DNA content of BS (peak1 : 58.14). K: Chromosome speads of BS2n= 48. L: The karyotype of BS, 24 m+ 20sm+ 4st. Bar = 10 μm.

3.4. Identification and analysis of microsatellite in CE

Building upon the initial screening of TTF-3, TTF-20, and TTF-32 via PAGE, this study further validated the reliability of these three diagnostic primers using CE technology. The results confirmed their precise discriminative capacity for BSB, SJF, and GDF populations (Fig. A2). Subsequently, the analysis was expanded to conduct SSR genotyping across 11 *Megalobrama* populations from diverse river systems using CE. Across four BSB populations of Hunan and Hubei founder stocks, Hunan cultured stock and wild population, TTF-3 invariably generated a 130 bp diagnostic fragment for BSB (Fig. 5A). In three GDF populations of Guangdong founder stock, cultured stock, Pearl River wild stock), TTF-



(caption on next page)

Fig. 4. PAGE profiles of TTF-3, TTF-20 and TTF-32 primers in the *Megalobrama* fish. A: TTF-3 PAGE profile in the founder stocks of BSB, SJF and GDF. B: TTF-20 PAGE profile in the founder stocks of BSB, SJF and GDF. C: TTF-32 PAGE profile in the founder stocks of BSB, SJF and GDF. D: TTF-3 PAGE profile in the wild population of BSB. E: TTF-32 PAGE profile in the wild population of BSB. 5,6,10,22 are speculated as BS in the BSB wild population. Note: M: PBR322 DNA/Msp I Standard molecular weight. In A-C, Lane 1–6: A GDF founder stock from Shaoguan Fishery Technology Extension Station in Guangdong , Lane 7–12: A SJF founder stock from Shaoguan Fishery Technology Extension Station in Guangdong, Lane 13–18: A BSB founder stock from Hunan Aquatic Germplasm Farm. In D-E, Lane 1–22: A BSB wild population from the Yueliangwan Section of the Xiangjiang River in Hunan. The red arrow indicates the diagnostic fragment that distinguishes BSB, the green arrow indicates the diagnostic fragment that distinguishes GDF, the blue arrow indicates the diagnostic fragment that distinguishes SJF, and the purple arrow indicates the specific amplified fragment that distinguishes BS.

20 produced a 125-bp GDF-specific fragment (Fig. 5B). Among four SJF populations of Hunan and Guangdong founder stocks, Guangdong cultured stock, Hubei wild population, TTF-32 consistently amplified a 100-bp SJF-specific fragment (Fig. 5C). These findings by CE demonstrated consistent species-specific amplification, and verified the cross-population applicability and stability of these markers for the *Megalobrama* differentiation (Fig. 5).

Critically corroborating the PAGE results, all seven morphologically distinct BS individuals, identified from the Xiangjiang River BSB wild population ($n = 36$), exhibited concurrent amplification of both the 130 bp BSB-specific fragment with TTF-3 (Fig. 6A) and the 100 bp SJF-specific fragment with TTF-32 (Fig. 6B). This molecular evidence conclusively confirms these individuals as hybrids originated from the hybridization event between *M. amblycephala* and *M. terminalis*.

3.5. Feeding habits and growth performance

Under controlled thermal regimes, SJF consistently demonstrated superior feeding performance. At 19.4 ± 2.3 °C, its duckweed consumption rate (13.88% ± 0.42%) significantly exceeded GDF (6.29% ± 1.28%), BS (4.70% ± 1.05%), and BSB (4.39% ± 1.36%) by 228.78% ± 39.88%, 308.73% ± 30.03%, 346.46% ± 46.76%, respectively ($P < 0.05$). At 14.1 ± 1.9 ℃, SJF (11.57% ± 0.43%) maintained feeding superiority, outperforming GDF (4.93% ± 0.70%), BS (2.90% ± 0.80%), and BSB (2.60% ± 1.03%) by 238.49% ± 25.27%, 472.30% ± 102.78%, and 523.13% ± 191.95% ($P < 0.05$) (Fig. 7A). Furthermore, at 20.8 ± 2.9 ℃, its commercial feed consumption rate (2.24% ± 0.25%) significantly surpassed GDF (1.30% ± 0.09%), BS (1.24% ± 0.09%), and BSB (1.09% ± 0.05%) by 171.80% ± 7.33%, 180.13% ± 7.09%, and 204.88% ± 13.54% ($P < 0.05$) (Fig. 7B). At 13.1 ± 2.4 ℃, SJF (1.52% ± 0.22%) exceeded its counterparts GDF (0.98% ± 0.17%), BS (0.94% ± 0.14%), BSB (0.84% ± 0.09%) by 155.27% ± 4.26%, 160.79% ± 0.47%, and 180.05% ± 7.36% ($P < 0.05$) (Fig. 7B).

Growth performance of BSB, SJF, GDF, and BS from July 2023 to October 2023 were recorded (Fig. 8A,B). SJF achieved highest weight gain (69.22% ± 3.91%), significantly exceeding GDF (31.40% ± 1.50%), BS (24.95% ± 3.31%), and BSB (17.84% ± 2.78%) by 220.37% ± 11.91%, 280.31% ± 21.54%, and 394.20% ± 39.54% ($P < 0.05$), though BSB showed maximal CF (1.45 ± 0.23 g/cm^3), significantly greater than BS (1.29 ± 0.17 g/cm^3), GDF (1.00 ± 0.09 g/cm^3), and SJF (0.92 ± 0.05 g/cm^3) by 112.00% ± 3.07%, 144.10% ± 10.03%, and 156.71% ± 16.48% (Fig. 8C).

Critically, the self-crossing offspring of hybrid BS individuals displayed intermediate feeding-growth traits, significantly surpassing BSB but underperforming SJF, validating their transitional phenotype between parental species.

3.6. Low temperature and high temperature tolerance

Low-temperature tolerance trials revealed that all fish populations exhibited normal activity when water temperature decreased to 4.5 °C, but as temperatures continued to drop, the fish began to swim slowly and react sluggishly. Between 4.0–4.2 °C, BSB and GDF sequentially showed initial stress responses. At 3.6–3.9 °C, GDF, BSB, and BS progressively lost balance, and within 2.4–3.5 °C, GDF, BSB, and BS successively experienced body tilting, with significant differences observed among all groups ($P < 0.05$) (Fig. 9A). The LT_{LD50} values were approximately 1.63 °C for GDF, 1.38 °C for BSB, 1.13 °C for BS, and 0.25 °C for SJF (Fig. 9B). Moreover, during cold stress, BS exhibited hyperactivity and experienced body tilting without supplemental aeration, whereas SJF maintained a relatively calm state throughout cooling, showing only slight reactions at 1.2 °C, and retained balance without tilting even in 0 °C ice-water mixtures, surviving for over 30 min under experimental conditions.

High-temperature tolerance experiments showed normal fish activity up to 27 °C, but beyond this threshold, accelerated swimming and hyperactive behavior emerged. GDF reacted first at 27.9 °C, followed sequentially by BSB, BS, and SJF around 28.2 °C. Loss of equilibrium occurred progressively in GDF, BSB, BS, and SJF between 28.3–29.2 °C. GDF displayed initial body tilting at 29.3 °C, while BSB, BS, and SJF successively tilted between 30.2–30.7 °C (Fig. 9C). HT_{LD50} values were approximately 30.37°C for GDF, 30.63°C for BSB, 30.99°C for BS, and 32.36°C for SJF (Fig. 9D). Remarkably, SJF manifested extreme hyperactivity under heat stress, contrasting sharply with its calm cold-response, while other populations showed similar hyperactivity in both cold and heat stress. Temperature tolerance trials confirmed that the self-crossing offspring of hybrid BS identified displayed intermediate tolerance between SJF and BSB, exhibiting higher tolerance than BSB but lower than SJF.

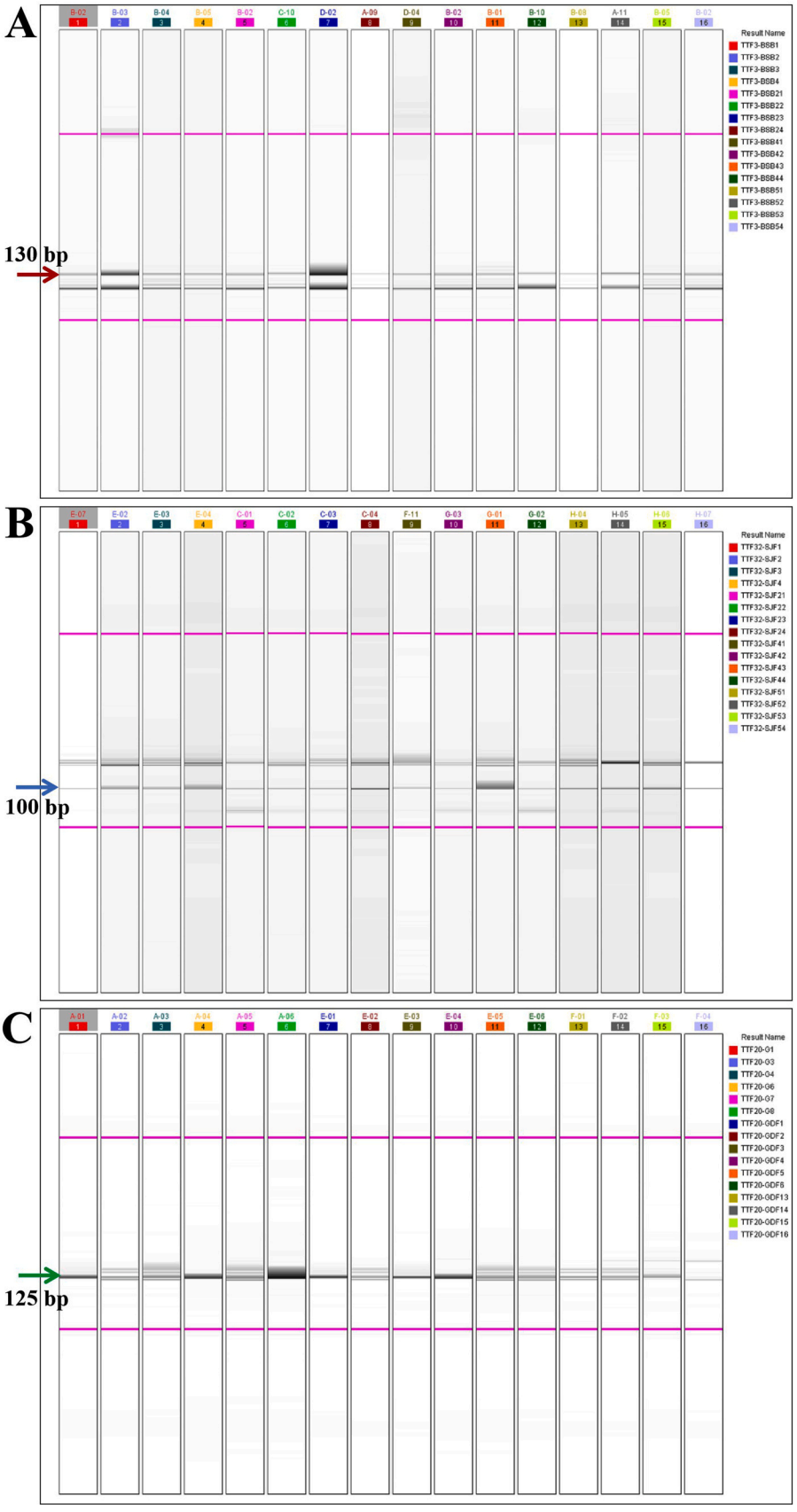
3.7. Hypoxia tolerance

Hypoxia tolerance tests revealed normal fish activity until DO decreased to 2.0 mg/L, but further DO reduction induced slowed swimming. At 1.9 mg/L, GDF first lost balance followed by tilting at 1.6 mg/L, while BSB exhibited balance loss at 1.5 mg/L and tilting at 1.3 mg/L, BS lost balance at 1.4 mg/L and tilted at 1.2 mg/L, and SJF displayed balance loss at 1.2 mg/L and tilting at 1.1 mg/L (Fig. 10A). The hypoxic DO_{LD50} values were approximately 1.62 mg/L for GDF, 1.29 mg/L for BSB, 1.12 mg/L for BS, and 0.92 mg/L for SJF (Fig. 10B). SJF underwent body tilting at dissolved oxygen levels of merely 91.7% ± 2.0% of BS, 84.6% ± 3.0% of BSB, and 68.8% ± 1.0% of GDF. Moreover, under 0.9–1.1 mg/L DO conditions, SJF survived for ~4 h before tilting, with its hypoxia tolerance duration exceeding that of BS by 266.7% ± 2.0%, BSB by 398.0% ± 3.0%, and GDF by 688.0% ± 5.0%.

The self-crossing offspring from BS individuals identified in this study exhibited intermediate hypoxia tolerance between SJF and BSB, specifically higher than BSB but lower than SJF, which aligns with findings from morphological, cytogenetic, microsatellite, feeding and growth performance, and temperature tolerance analyses, collectively verifying their hybrid origin between *M. amblycephala* and *M. terminalis*.

4. Discussion

The *Megalobrama* fish hold significant importance among China's economic fish, where maintaining stable genetic traits and conserving germplasm resources are crucial for their sustainable aquaculture. Regarding taxonomic classification, two primary perspectives exist domestically. The first, proposed by Bolu Yi and Qingjiang Wu, recognizes four species, *M. terminalis*, *M. amblycephala*, *M. hoffmanni*, and *M. pellegrini,* with *M. terminalis* inhabiting the Yangtze, Yellow, and Amur River basins, while *M. hoffmanni* occupies the Pearl River and Hainan Island drainages (Wu, 1964; Yi, 1955). The second perspective,



(caption on next page)

Fig. 5. CE profiles of TTF-3, TTF-20 and TTF-32 primers in different populations of the *Megalobrama* fish. A: CE profile of TTF-3 in different populations of BSB. Lane 1–4: A BSB founder stock from Hunan Aquatic Germplasm Farm, Lane 5–8: A BSB founder stock from the Hubei Wuchang Fish Germplasm Farm, Lane 9–12: A BSB cultured stock from the Datong Lake Fishery Farm in Hunan, Lane 13–16: A BSB wild population from the Yueliangwan Section of the Xiangjiang River in Hunan. B: CE profile of TTF-32 in different populations of SJF. Lane 1–4: A SJF founder stock from the Shaoguan Fishery Technology Extension Station in Guangdong, Lane 5–8: A SJF founder stock from Hunan Aquatic Germplasm Farm, Lane 9–12: A SJF cultured stock Nanshui Reservoir in Guangdong, Lane 13–16: A SJF wild population from the Jianli Section of the Yangtze River in Hubei. C: CE profile of TTF-20 in different populations of GDF. Lane 1–6: A GDF founder stock from the Shaoguan Fishery Technology Extension Station in Guangdong, Lane 7–12: A GDF cultured stock from the Nanshui Reservoir in Guangdong, Lane 13–16: A GDF wild population from the Humen Section of the Pearl River in Guangdong. Note: The red arrow indicates the diagnostic fragment that distinguishes BSB, the blue arrow indicates the diagnostic fragment that distinguishes SJF, and the green arrow indicates the diagnostic fragment that distinguishes GDF.

advocated by Yunlin Luo, also identifies four specie, *M. skolkovii*, *M. terminalis*, *M. amblycephala*, and *M. pellegrini*, but designates *M. terminalis* to the Pearl River and Hainan Island, with *M. skolkovii* distributed in the middle-lower Yangtze, Amur, and other basins (Chen, 1998; Luo, 1990). This study adheres to the first nomenclature system (Yi and Wu' s classification).

Morphological differentiation serves as a classical and traditional method for fish identification (Siong, 2016). The *Megalobrama* fish exhibit laterally compressed and deep bodies, small terminal mouths, short blunt snouts, variably developed keratinized jaws, a distinct abdominal ridge between the pelvic and anal fins, and a three-chambered swim bladder with the posterior chamber being smallest (Chen, 1998; Luo, 1990; Wu, 1964). This study collected 11 populations of *M. amblycephala*, *M. terminalis*, and *M. hoffmanni* from Hunan, Hubei, and Guangdong in China. Building upon prior taxonomic frameworks, we conducted detailed morphological identification using three diagnostic characteristics, body shape, swim bladder, and scale pigmentation. BSB possesses a high dorsal profile and longitudinal dark stripes, SJF displays a larger mouth, triangular-shaped body, and a swim bladder with the anterior chamber larger than the middle chamber, unlike BSB and GDF where the anterior chamber is smaller. GDF exhibits an elongated caudal peduncle and distinctive dark basal spots on lateral scales. Overall, BSB and SJF demonstrate minimal external morphological divergence, while GDF shows lower similarity to both. These characteristics provide critical identification markers for germplasm evaluation and selective breeding. During morphological surveys in the BSB wild population from Xiangjiang River (Yueliangwan section, Hunan), we identified seven atypical individuals designated BS that diverged from the three established species. These specimens displayed intermediate measurable traits between BSB and SJF, including body height, head length, eye diameter, caudal peduncle height, and caudal fin length, with closer affinity to SJF. Their swim bladder configuration aligned with BSB (middle chamber > anterior chamber). We preliminarily hypothesize these individuals represent a hybrid population between distinct *Megalobrama* species.

DNA content and karyotype serve as foundational elements in cytogenetic research, reflecting species' genetic characteristics and providing critical evidence for determining phylogenetic relationships among taxa (Wang et al., 2021; Zhu and Pan, 2022). Pioneering work by Zan et al. (1979) first documented the chromosome karyotype of *Megalobrama amblycephala* using embryonic cell preparation (Zan and Song, 1979), followed by Yu et al. (1989) reporting chromosomal studies on > 200 freshwater fish species in China via head kidney cell preparation (Yu et al., 1989). Systematically analyzing five species, *M. amblycephala*, *M. hoffmanni*, *M. terminalis*, *M. pellegrini*, and *Parabramis pekinensis*, Wu et al. (2015) established their karyotypes by kidney cell method and DNA content by peripheral blood cell measurement, elucidating the evolutionary status of *Megalobrama* and *Parabramis* species (Wu et al., 2015). This study investigates contemporary cytogenetic features and evolutionary dynamics of *Megalobrama* through karyotyping and DNA content analysis. All the populations are diploid with 2 n = 48 chromosomes, aligning with Wu's findings (Wu et al., 2015). Notably, BS shares an identical karyotype with BSB and SJF, 24 m+ 20sm+ 4st, exhibiting one fewer metacentric pair and one additional submetacentric pair compared to GDF (Fig. 3).

To address the challenge of morphological convergence in early developmental stages of the *Megalobrama* species, which impedes accurate identification through conventional morphological methods alone, this study developed three microsatellite markers, TTF-3, TTF-20, TTF-32, through transcriptome high-throughput sequencing, polyacrylamide gel electrophoresis, and capillary electrophoresis. Meanwhile, this study validated the applicability and stability of three specific microsatellite primer pairs across 11 distinct *Megalobrama* populations spanning multiple river basins. Microsatellite analysis revealed minimal genetic divergence between *M. amblycephala* and *M. terminalis*, while *M. hoffmanni* exhibited greater genetic distance from both, aligning with morphology assessments and corroborating prior mitochondrial genome amplification studies. For instance, Hu et al. (2019) reported distant phylogeny between *M. terminalis* and *M. hoffmanni* (Hu et al., 2019). Notably, atypical BS individuals, morphologically distinct from BSB, SJF, and GDF, amplified both BSB-specific and SJF-specific bands, suggesting their hybrid origin between *M. amblycephala* and *M. terminalis*. These findings confirm the utility of the three markers for rapid discrimination of *Megalobrama* species and hybrids (Figs. 4,5). The established germplasm identification protocol, integrating high-throughput sequencing with capillary electrophoresis, prevents misidentification arising from morphological convergence. Compared to traditional magnetic bead and linkage mapping methods, this approach significantly enhances the throughput and efficiency of microsatellite screening while ensuring operational feasibility and high accuracy.

Beyond morphological and molecular genetic markers, growth performance and stress resistance serve as fundamental criteria for germplasm evaluation, and particularly critical indicators for selective breeding of superior varieties. Feeding efficiency and growth performance constitute vital economic traits in aquaculture, with documented practices in China's freshwater farming utilizing duckweed for rearing *Megalobrama* broodstock or adults (Guo et al., 2024). This study systematically compared duckweed and commercial pellet consumption across distinct *Megalobrama* populations under two temperature regimes using the food balance method. The results demonstrated that SJF consistently exhibited significantly higher daily feeding rates than other species regardless of diet, and all species showed enhanced feeding performance at optimal temperatures. Consumption at ~20°C substantially surpassed that below 15°C, aligning with Liang et al. (2024) (Liang et al., 2024). Growth monitoring during July to October 2023 revealed that despite smaller initial size, SJF displayed superior growth performance, outperforming others in weight gain rate and specific growth rate ($P < 0.05$). However, Luo and Xie (2008) attributed this inverse correlation between smaller body size and higher feeding rates primarily to elevated standard metabolic rates, increased energy expenditure, and consequently heightened appetite in diminutive individuals (Luo and Xie, 2008).

Environmental tolerance in fish refers to their survival capacity and adaptive mechanisms under adverse conditions, with water temperature and dissolved oxygen widely recognized as critical environmental factors influencing aquatic organisms' physiology and behavior. Under laboratory simulated stressors, this study observed interspecific variation in tolerance among *Megalobrama* species, with the hierarchy of SJF > BS > BSB > GDF. The markedly superior tolerance of SJF partially explains its broader natural distribution. Hybrid individuals exhibited intermediate performance between SJF and BSB, displaying inferior tolerance to SJF but superior to BSB in both growth and stress resistance.

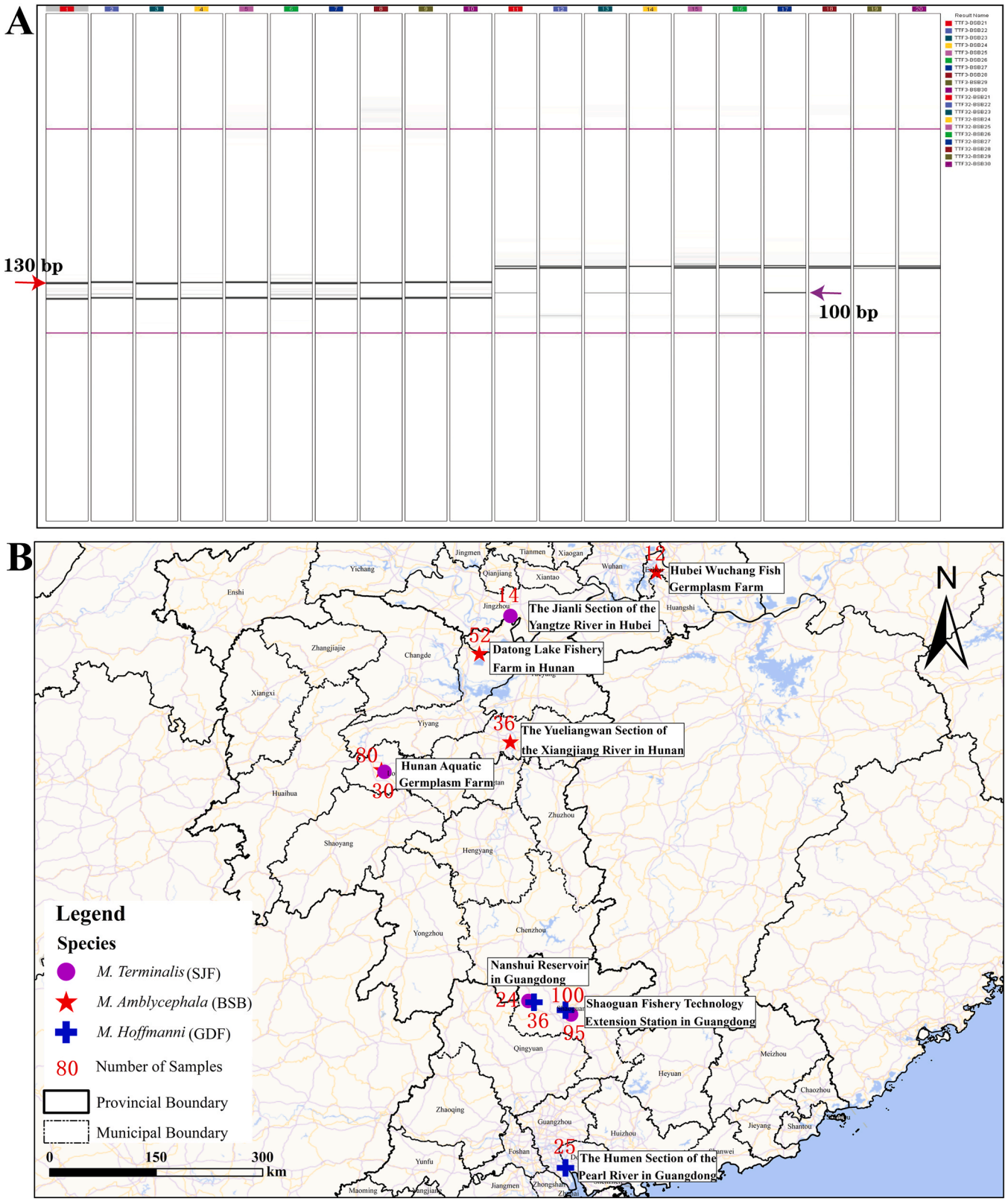


Fig. 6. Suspected hybrid individuals in the BSB wild population based on CE amplification profiles of TTF-3 and TTF-32. A: CE profiles of primers TTF-3 and TTF-32. Lanes 1–10: CE profiles of TTF-3 primer for BSB wild population, Lanes 11–20: CE profiles of TTF-32 primer for BSB wild population. Red arrows indicated the 130 bp BSB-specific amplification fragments, and purple arrows indicated the 100 bp SJF-specific amplification fragments. 11, 13, 14, 17 are speculated as BS in the BSB wild population. B: Distribution of the sampling locations for the *Megalobrama* fish. The Red box indicated the sampling location of the BSB wild population where hybrid-origin individuals were detected, namely the Yueliangwan Section of the Xiangjiang River in Hunan.

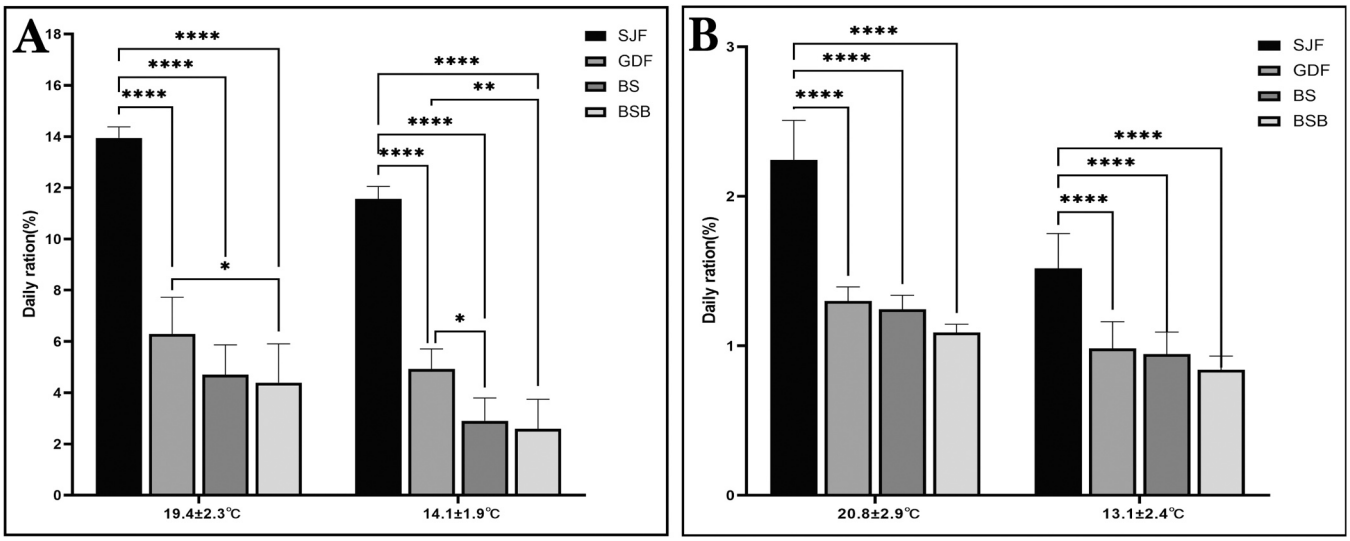


Fig. 7. The daily feeding rate of duckweed (A) and commercial feed (B) in the *Megalobrama* fish.

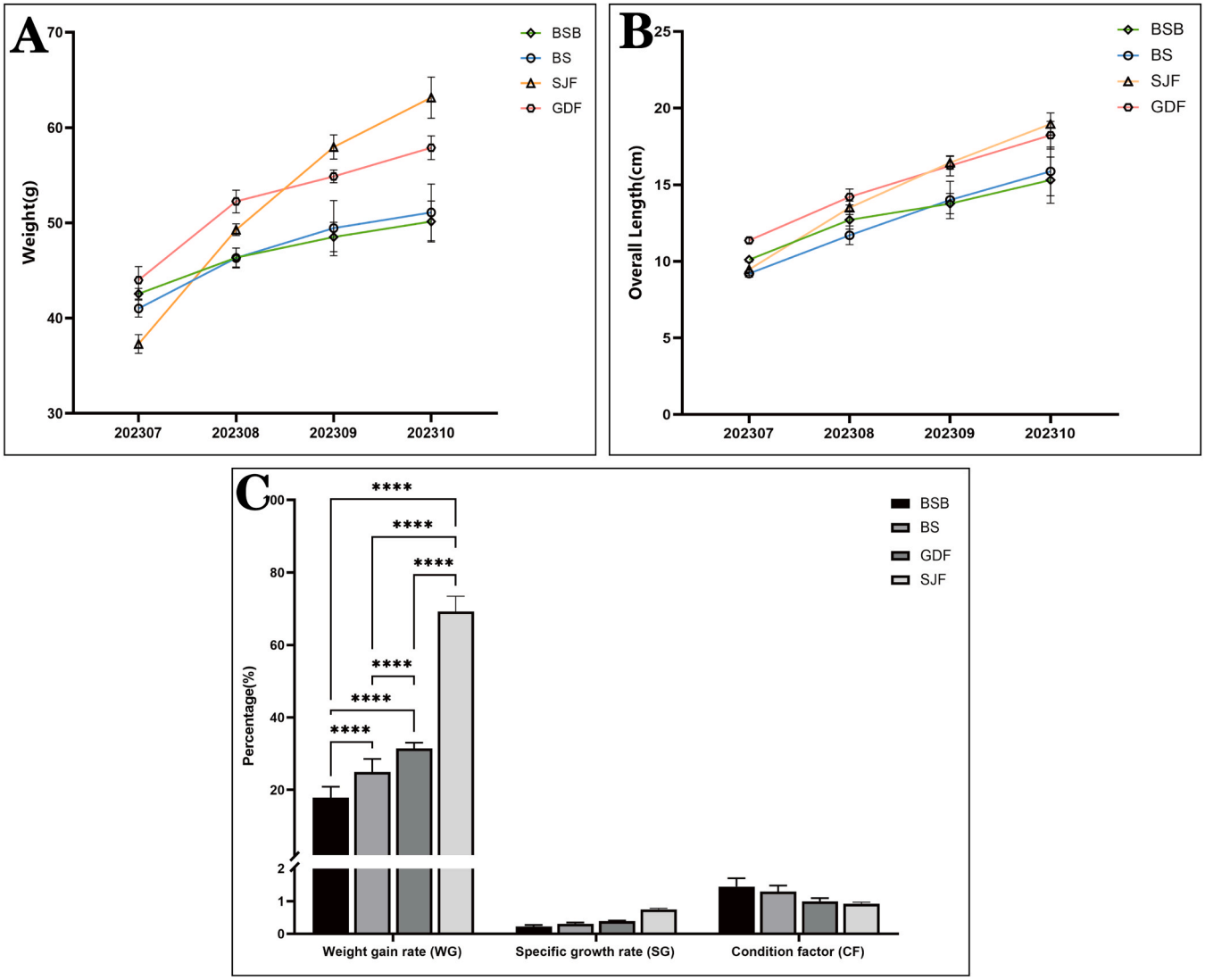


Fig. 8. Growth Performance of the *Megalobrama* fish. A: Weight gain from July to October 2023. B: Body length gain from July 2023 to October 2023. C: WG, SG and CF among the *Megalobrama* fish.

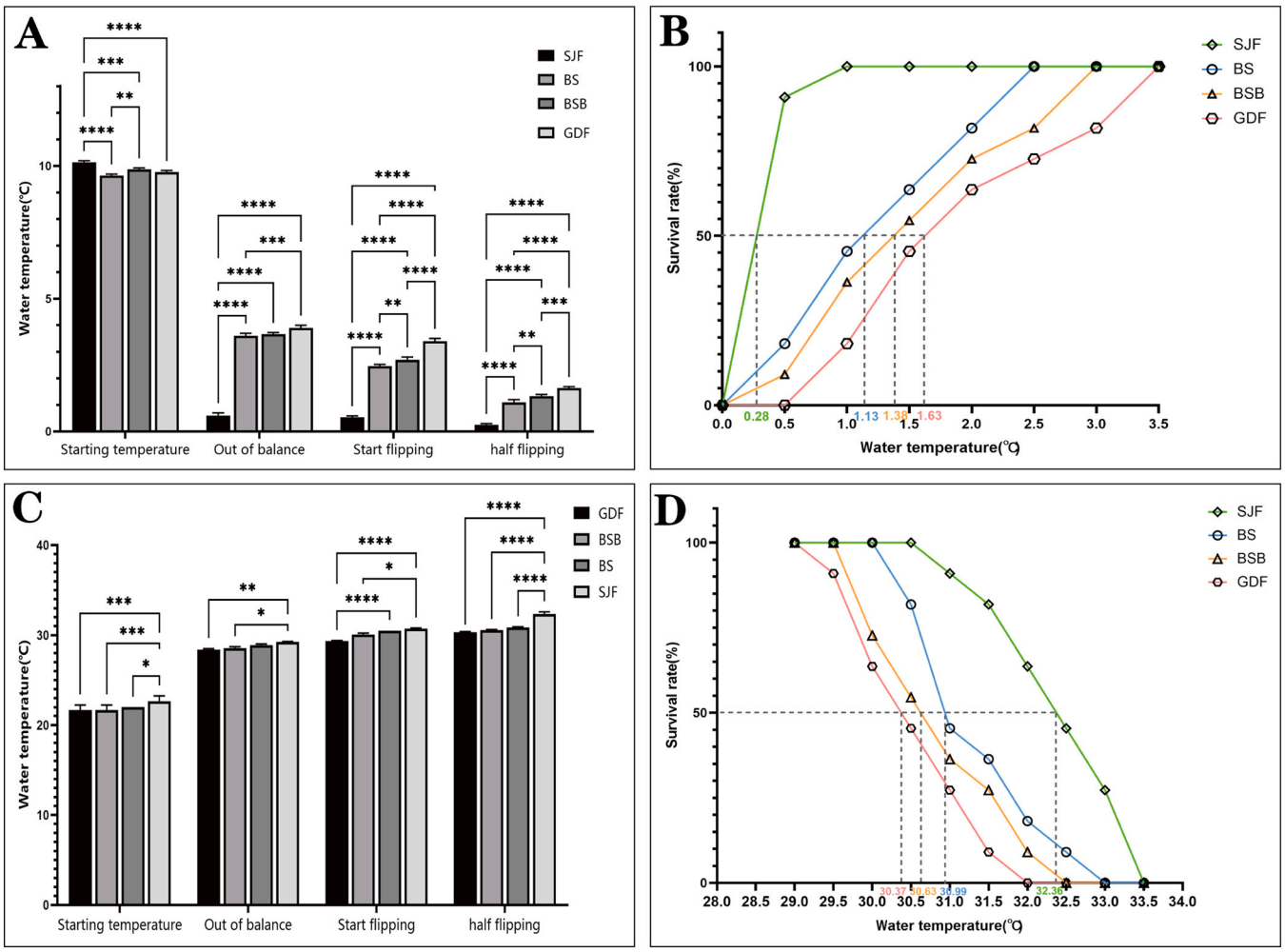


Fig. 9. Temperature tolerance of the *Megalobrama* fish. A: Low temperature tolerance in the *Megalobrama* fish. B: Low-temperature median lethal dosage ($LT_{LD_{50}}$). C: High temperature tolerance in the *Megalobrama* fish. D: High-temperature median lethal dosage ($HT_{LD_{50}}$).

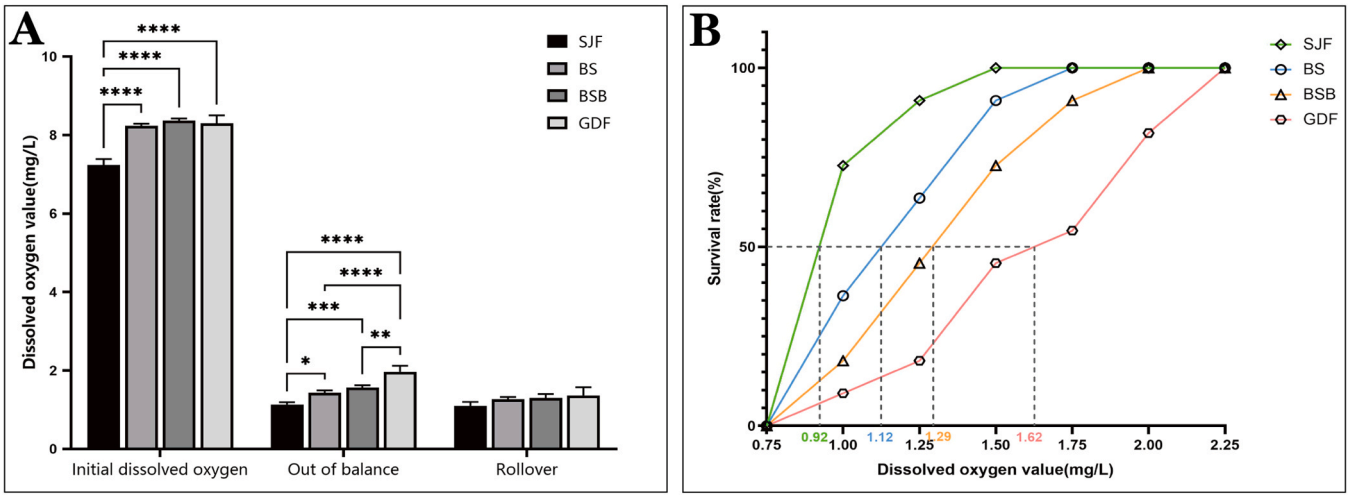


Fig. 10. Hypoxia tolerance (A) and dissolved-oxygen median lethal dosage ($DO_{LD_{50}}$). (B) in the *Megalobrama* fish.

These findings, combined with morphological characteristics, cytogenetic profiles, microsatellite markers, and feeding & growth performance, conclusively identifies them as hybrids originated from the hybridization event between *M. amblycephala* and *M. terminalis*, manifesting distinct heterosis.

Previous studies have documented individuals resembling "hybrid-like" in natural populations, with identification methods spanning morphological, physiological, biochemical, cytogenetic, and genomic approaches. Tilapiine Cichlids, the most extensively farmed freshwater fish, have experienced introductions into non-native ranges, triggering

hybridization that causes morphological and genetic homogenization, and erodes distinct population genetic structure (Canonico et al., 2005; Nehemia, 2025; Shechonge et al., 2018). Similarly, introduced rainbow trout (*Oncorhynchus mykiss*) readily hybridize with native Yellowstone cutthroat trout (*O. clarkii*) in western North America, resulting in genetic introgression, population decline. Currently, cutthroat trout persist in merely 44% of their historical range (Al-Chokhachy et al., 2018; Rosenthal et al., 2022). Furthermore, wild Japanese medaka (*Oryzias latipes*) populations comprise not only two genetically distinct groups, northern and southern populations, but also boundary populations with unique genotypes. Genome-wide single nucleotide polymorphism (SNP) analyses reveal these boundary populations originated from the northern population, followed by independent natural hybridization and recurrent backcrossing with southern populations (Takehana et al., 2016).

Hybrid offspring often exhibit traits intermediate between parental species or display transgressive phenotypes, providing a crucial source for adaptive evolution. For instance, a study on endemic rainbowfishes in the Wet Tropics bioregion of northeastern Australia revealed distinct biogeographic divergence in climate change adaptability among five closely related tropical species: one widespread lowland generalist (*Melanotaenia splendida splendida*) and four narrow range specialists (NERs). In recent decades, climate change has facilitated the continuous incursion of *M. splendida* into higher-elevation habitats occupied by NERs, with hybrid individuals documented in contact zones. The hybridization and introgression patterns between *M. splendida* and NERs indicate that introgressive hybridization may supply novel adaptive variation, potentially enabling evolutionary rescue of species threatened by climate change (Brauer et al., 2023). Generalist species with broader environmental tolerance ranges may possess greater resilience to rapid climate shifts. Through interspecific introgression achieved via repeated backcrossing to transfer genetic material between species, vulnerable species can acquire and utilize evolutionary components from better-adapted taxa (Brauer et al., 2023).

M. terminalis is widely distributed across the Yangtze, Yellow, and Amur River basins, representing the most extensively distributed species within the genus *Megalobrama*. Both historical reports and the current study demonstrate its superior environmental adaptability, which is supported by phylogeographic analyses revealing significant population expansions shaped by historical sea-level changes, underscoring its adaptive resilience (Chen et al., 2020). The natural distribution ranges of *M. terminalis* and *M. amblycephala* exhibit geographical overlap with no complete geographic isolation. Notably, their close phylogenetic relationship within the genus *Megalobrama* reduces potential post-zygotic barriers, making interspecific crossing genetically feasible. Consequently, the emergence of hybridization within this genus raises critical questions regarding its underlying mechanisms. First, it is essential to discern whether such hybridization represents independent, sporadic events or sustained interspecific introgression. This question is particularly pertinent given that natural hybridization is a documented and sometimes adaptive phenomenon among cyprinid fishes (Ren et al., 2025). Second, evaluating the primary drivers is crucial. Hybridization could be mainly driven by anthropogenic factors including stock enhancement programs and artificial breeding practices, which may artificially promote contact. Alternatively, it might arise from evolutionary adaptation to changing natural environments, where hybrid genotypes could offer selective advantages in altered habitats, as demonstrated by the role of asymmetric gene expression in dietary adaptation of hybrid fish (Li et al., 2021). Disentangling these intertwined possibilities, unique event versus ongoing gene flow, human-mediated versus natural selection, is key to understanding the evolutionary trajectory and conservation implications of hybridization in *Megalobrama*.

Furthermore, fundamental uncertainties persist regarding the hybrid specimens. Whether they represent intermediate forms during the speciation process of the *Megalobrama* fish, or constitute post-speciation hybridization events following complete diversification. These phylogenetic and mechanistic dimensions warrant further in-depth investigation.

5. Conclusion

The collection, identification, and preservation of fish germplasm resources serve to prevent species decline and extinction, facilitate the conservation of genetic diversity, advance selective breeding of superior varieties, and thereby establish foundations for sustainable germplasm utilization. This study gathered founder stocks, wild populations, and cultured stocks of *M. Amblycephala*, *M. Terminalis*, and *M. Hoffmanni* from distinct aquatic systems, with morphological analyses revealing individuals that diverged from the three primary *Megalobrama* species in wild *M. amblycephala* populations. Comprehensive comparisons of cytogenetic characteristics, microsatellite DNA markers, growth performance metrics, and environmental tolerance thresholds further suggested these individuals to be hybrids between *M. amblycephala* and *M. terminalis*. These findings establish critical germplasm authentication benchmarks for addressing current genetic admixture issues in Chinese *Megalobrama* fisheries, while providing novel perspectives for biodiversity conservation and ecological equilibrium maintenance.

CRediT authorship contribution statement

Jie Hu: Writing – review & editing, Writing – original draft, Validation, Resources, Project administration, Methodology, Data curation. **Shaojun Liu:** Project administration. **Jie Yang:** Writing – review & editing, Writing – original draft, Validation, Methodology, Data curation. **Li Zou:** Resources. **Siyu Fan:** Resources. **Min Tao:** Resources. **Chun Zhang:** Resources.

Declaration of Competing Interest

The authors declare that they have no known competing financial interests or personal relationships that could have appeared to influence the work reported in this paper.

Acknowledgements

This research was supported by the National Key R&D Program of China (Grant No. 2022YFD2400601), the National Natural Science Foundation of China (Grant No. 32293250) and the Pearl River S&T Nova Program, Science and Technology Project of Guangzhou (Grant No. 201906010025).

Appendix A. Supporting information

Supplementary data associated with this article can be found in the online version at doi:10.1016/j.aqrep.2026.103591.

Data availability

No data was used for the research described in the article.

References

Al-Chokhachy, R., Shepard, B.B., Burckhardt, J.C., Garren, D., Opitz, S., Koel, T.M., Nelson, L., Gresswell, R.E., 2018. A portfolio framework for prioritizing conservation efforts for Yellowstone cutthroat trout populations. Fisheries 43 (10), 485–496.

Blödorn, E.B., Domingues, W.B., Nunes, L.S., Komninou, E.R., Pinhal, D., Campos, V.F., 2021. MicroRNA roles and their potential use as selection tool to cold tolerance of domesticated teleostean species: a systematic review. Aquaculture 540.

Brauer, C.J., Sandoval-Castillo, J., Gates, K., Hammer, M.P., Unmack, P.J., Bernatchez, L., Beheregaray, L.B., 2023. Natural hybridization reduces vulnerability to climate change. Nat. Clim. Change 13 (3) 282-289.

Bureau of Fisheries, M.o.A.a.R.A., People's Republic of China, 2024. China Fisheries Statistical Yearbook 2024, 2024, Beijing: China Agriculture Press.

C.L, H., K.F, L., 1964. Fishes of the Great Lakes Region, 1964. University of Michigan Press.
Cai, M.J., Zhang, M.Y., Zeng, Q.L., Liu, H.Z., 2001. A study on morphometrics of the genus *Megalobrama*. Acta Hydrobiol. Sin. 25 (06), 631–635.
Canonico, G.C., Arthington, A., McCrary, J.K., Thieme, M.L., 2005. The effects of introduced tilapias on native biodiversity. Aquat. Conserv. Mar. Freshw. Ecosyst. 15 (5), 463–483.
Chen, Y.Y., 1998. Fauna sinica-osteichthyes *Cypriniformes* II. Beijing. Sci. Technol. Press 200–208.
Chen, W.T., Li, C., Chen, F.C., Li, Y.F., Yang, J.P., Li, J., Li, X.F., 2020. Phylogeographic analyses of a migratory freshwater fish (*Megalobrama terminalis*) reveal a shallow genetic structure and pronounced effects of sea-level changes. Gene, 144478.
Chen, J., Li, F.G., Huang, C.X., Jiang, X.Y., Zou, S.M., 2014. Morphological variations of genera *Parabramis* and *Megalobrama* teleost populations. J. Shanghai Ocean Univ. 23 (03), 388–394.
Chen, J., Wang, W.M., 2021. Genetic diversity and genetic differentiation of *Megalobrama* populations inferred by mitochondrial markers. Genes Genom. 43 (10), 1119–1132.
Feng, X.Y., 2009. Research progress and demonstration extension of *Megalobrama terminalis* in Zhejiang Province. Sci. Fish. Farming 10, 40–41.
Gao, Z.X., Luo, W., Liu, H., Zeng, C., Liu, X.L., Yi, S.K., Wang, W.M., 2012. Transcriptome analysis and SSR/SNP markers information of the blunt snout bream (*Megalobrama amblycephala*). PLoS. One 7 (8), e42637.
Gao, Z.X., Wang, W.M., Jiang, E.M., Chen, B.X., 2014. Research advances on germplasm resources and genetic improvement of blunt snout bream(*Megalobrama amblycephala*). Huazhong Agric. Univ. 33 (03), 138–144.
Gong, D.B., Xu, L.H., Li, W.H., Shang, R.J., Chen, J.X., Hu, F.Z., Wang, S., Liu, Q.F., Wu, C., Zhou, R., Zhang, C., Tao, M., Wang, Y.Q., Liu, S.J., 2020. Comparative analysis of liver transcriptomes associated with hypoxia tolerance in the gynogenetic blunt snout bream. Aquaculture 523, 735163.
Guo, Y.S., Liu, W.C., Xiao, D.D., Zhang, S.H., Li, Z.F., Luo, K.F., Luo, G.Z., Tan, H.X., 2024. A novel multitrophic biofloc technology for duckweed and *Megalobrama amblycephala* integrated culture: improving nutrient utilization and animal welfare. Sci. Total Environ. 934, 173239.
Hamada, H., Petrino, M.G., Kakunaga, T., 1982. A novel repeated element with Z-DNA-forming potential is widely found in evolutionarily diverse eukaryotic genomes. Proc. Natl. Acad. Sci. Usa. 79 (21), 6465–6469.
Hu, J., Liu, S., Xiao, J., Zhou, Y., You, C., He, W., Zhao, R., Song, C., Liu, Y., 2012. Characteristics of diploid and triploid hybrids derived from female Megalobrama amblycephala Yih × male Xenocypris davidi Bleeker. Aquaculture 364-365, 157–164.
Hu, X.S., Luan, P.X., Cao, C.H., Li, C., Jia, Z., Ge, Y., Shang, M., Wang, S., Meng, Z., Tong, J., Shi, L., 2019. Characterization of the mitochondrial genome of *Megalobrama terminalis* in the Heilong River and a clearer phylogeny of the genus *Megalobrama*. Sci. Rep. 9 (1), 8509.
Hu, J., Yang, J., Liao, H., 2024. Progress on stress resistance breeding in fish. Reprod. Breed. 4 (4), 267–278.
Kraitavin, W., Yoshitake, K., Igarashi, Y., Mitsuyama, S., Kinoshita, S., Kambayashi, D., Watabe, S., Asakawa, S., 2019. Transcriptome Analysis of Yamame (*Oncorhynchus masou*) in normal conditions after heat stress. Biology 8 (2), 21.
Li, L., Li, X.H., Yang, J.P., Li, Y.F., Li, J., Shuai, F.M., Zhu, S.L., 2014. Establishment of microsatellite identification on there Culterinae fishes in Pearl River. Guangdong Agric. Sci. 41 (10), 102–105. +110.
Li, W.T., Liao, X.L., Yu, X.M., Wang, D., Tong, J., 2007b. Isolation and characterization of polymorphic microsatellite loci in Wuchang bream (*Megalobrama amblycephala*). Mol. Ecol. Notes 7 (5), 771–773.
Li, W.H., Wang, S., Hu, J., Tang, C.C., Wu, C., Liu, J.M., Li, Ren, Sun, C.F., Dong, J.J., Liu, S.J., Ye, X., 2021. Asymmetric expression of homoeologous genes contributes to dietary adaption of an allodiploid hybrid fish derived from Megalobrama amblycephala (♀) × Culter alburnus (♂). BMC Genom. 22 (1).
Li, W.J., Wang, J.W., Xie, C.X., Tan, D.Q., 2007a. Age structure and growth characteristiics of *Megalobrama pellegrini* an endemicfish living only in upper reaches of Yangtze River. J. Fish. Sci. China 02, 215–222.
Li, S.F., Zhu, Z.W., Zou, S.M., Zhao, J.L., Cai, W.Q., 2002. Interspecific Phylogenesis and intraspecific genetic differencesofgenus *Megalobrama*: bluntnose black bream (*M. amblycephala*), guangdong black bream (*M. hoffmanni*) and black bream (*M. terminalis*). Curr. Zool. 03, 339–345.
Liang, Z.W., Li, W.Y., Yin, X.L., Xu, X., Sun, W.J., Wang, X.E., Chen, C.Y., Liao, Z., Yan, X. J., Zhang, X.L., 2024. Effect of temperature on feeding rate and gill cilia of *Mytilus coruscus*. J. Oceanol. Limnol. 55 (02), 471–478.
Liu, S.J., 2015. Fish Distant Hybridization, 2015. Science Press, Beijing.
Luo, Y.L., 1990. A revision of fishes of the cyprinid genus *Megalobrama*. Acta Hydrobiol. Sin. 14 (02), 160–165.
Luo, Y.P., Xie, X.J., 2008. Effects of temperature on the specific dynamic action of the southern catfish, *Silurus meridionalis*. Comp. Biochem. Physiol. Part A Mol. Integrative Physiol. 149 (2), 150–156.
Manish, K., Pooja, M., Vikas, S., Chand, G.R., 2020. Analysis of genetic diversity and population structure in *Asparagus* species using SSR markers. Genet. Eng. Biotech. 18 (1), 50-50.
Nehemia, A., 2025. Genetic variation and lack of hybridization in five cichlid fish species in the Malagarasi River basin, Tanzania. Ecol. Genet. Genom. 35, 100355.
Oliya, B.K., Kim, M.Y., Lee, S.H., 2018. Development of genic-SSR markers and genetic diversity of Indian lettuce (*Lactuca indica* L.) in South Korea. Genes Genom. 40 (6), 615–623.
Pan, J.H., 1991. The freshwater fishes of GuangDong province. GuangDong Science and technoligy press, GuangDong.
Pan, R.J., Guo, Z.Z., Xu, W.Y., Li, S.S., Zheng, G., Zou, S.M., 2023. Cooperative adaptation strategies of different tissues in blunt snout bream (*Megalobrama amblycephala*) juvenile to acute ammonia nitrogen stress. Environ. Sci. Pollut. Res. Int. 30 (40), 92042–92052.
Ren, L., Tu, X.L., Luo, M.X., Liu, Q., Cui, J., Gao, X., Zhang, H., Tai, Y., Zheng, Y., .Li, M., Wu, C., Li, W., Wang, J., Wu, D., Liu, S.J., 2025. Genomes reveal pervasive distant hybridization in nature among cyprinid fishes. Gigascience 14, 000.
Rosenthal, W.C., Fennell, J.M., Mandeville, E.G., Burckhardt, J.C., Walters, A.W., Wagner, C.E., 2022. Hybridization decreases native cutthroat trout reproductive fitness. Mol. Ecol. 31 (16), 4224–4241.
Seephua, N., Bunyatratchata, A., Chumroenphat, T., Thammapat, P., Chaikwang, T., Siriamornpun, S., 2025. Nutritional composition and bioactive profiles of farmed and wild watermeal (Wolffia globosa). Foods 14 (10), 1832.
Shechonge, A., Ngatunga, B.P., Tamatamah, R., Bradbeer, S.J., Harrington, J., Ford, A.G. P., Turner, G.F., Genner, M.J., 2018. Losing cichlid fish biodiversity: genetic and morphological homogenization of tilapia following colonization by introduced species. Conserv. Genet 19 (5), 1199–1209.
Shen, X.Y., Kwan, H.Y., Thevasagayam, N.M., Prakki, S.R., Kuznetsova, I.S., Ngoh, S.Y., Lim, Z., Feng, F., Chang, A., Orbán, L., 2014. The first transcriptome and genetic linkage map for Asian arowana. Mol. Ecol. Resour. 14 (3), 622–635.
Singh, R.B., Mahenderakar, M.D., Jugran, A.K., Singh, R.K., Srivastava, R.K., 2020. Assessing genetic diversity and population structure of sugarcane cultivars, progenitor species and genera using microsatellite (SSR) markers. Gene 753, 144800.
Siong, W., 2016. Studies on morphology and genetic structure of the genus *Megalobrama* and *Parabramis*. Huazhong Agric. Univ.
Song, W., Wang, Y.Z., Zhu, D.H., Ren, L., Wang, W.D., 2013a. Morphological variations among the genus *Megalobrama*. Freshw. Fish. 43 (03), 21–27.
Song, W., Wang, Y.Z., Zhu, D.M., Nie, Z.L., Wang, W.M., 2013b. Morphological variation and discriminant analysis of three geographical populations of freshwater bream *Megalobrama skolkovii*. Chin. J. Fish. 26 (04), 1–7.
Takata, R., Mattioli, C., Bazzoli, N., Corrêa-Junior, J., Kennedy, L., 2021. The effects of salinity on growth, gill tissue and muscle cellularity in *Lophiosilurus alexandri* juvenile, a Neotropical freshwater catfish. Aquac. Res. 52 (3), 4064–4075.
Takehana, Y., Sakai, M., Narita, T., Sato, T., Naruse, K., Sakaizumi, M., 2016. Origin of boundary populations in Medaka (*Oryzias latipes* Species Complex). Zool. Sci. 33 (2), 125–131.
Tang, S.J., Li, S.F., Cai, W.Q., 2009. Development of microsatellite markers for blunt snout bream *Megalobrama amblycephala* using 5′-anchored PCR. Mol. Ecol. Resour. 9 (3), 971–974.
Thongthung, H., Chungopast, S., Petchpoung, K., Kaewtapee, C., 2024. Chemical composition and in vitro protein digestibility of duckweed and feed ingredients. Trends Sci. 21 (11).
Wang, H., Fu, Y., Gu, P., Zhang, Y., Tu, W., Chao, Z., Wu, H., Cao, J., Zhou, X., Liu, B., Michal, J.J., Fan, C., Tan, Y., 2020. Genome-wide characterization and comparative analyses of simple sequence repeats among four miniature pig breeds. Animals 10 (10).
Wang, Q.H., Liu, Z.W., Zhen, W., Zhang, X.M., Hao, Z., Mo, J., Zhao, X.F, Y., 2019. Effects of different densities of Wuchang bream on community structure of *Hydrilla verticillata* and *Vallisneria denseserrulata*. J. Lake Sci. 31 (03), 862–868.
Wang, X., Ma, H., Zhu, D.M., Sun, N., Li, Q., Wang, G.Y., Chen, J., Sun, Y.H., Li, P., 2021. Karyotype and Cellular DNA Contents of Culter Hybrid F_1 *Erythroculter ilishaeformis* (♀) x *Ancherythroculter nigrocauda*(♂), "Xianfeng No. 1". Fish. Sci. 40 (03), 347–353.
Wu, X.W., 1964. *Chinese Cyprinidae Fish Flora*(Upscroll). ShangHai Scientific & Technical Publishers, pp. 93–97.
Wu, C.B., Li, F.G., Chen, J., Jiang, X.Y., Zou, S.M., 2015. Karyotype and DNA contents analysis of *Parabramis* and *Megalobrama*. J. Shanghai Ocean Univ. 24 (06), 801–809.
Xu, W., Xiong, B.X., 2008. Advances in the Research on Genus Megalobrama in China. Hydroecology 29 (06), 7–11.
Yan, C.X., Liang, L.Q., Sun, X.W., Cao, D.C., 2007. Comparison of the morphological characteristics between two types of backcross progenies from the common and crucian carp. Northeast Agric. Univ. 06, 797–800.
Yi, B.L., 1955. Notes on *Megalobrama amblycephala*,SP.NOV., A distinct species from *M. terminalis*(Richardson). Acta Hydrobiol. Sin. 02, 115–122.
Yu, X.J., Zhou, D., Li, K., 1989. Chinese freshwater fish chromosomes, 1989. China Science Publishing & Media Ltd, Beijing.
Zan, R.G., Song, Z., 1979. Analysis and comparison between the karyotypes of *Ctenopharyngodon idellus* and *Megalobrama amblycephala*. Genes Genom. 02, 205–210. +241.
Zeng, C., Yan, L.Q., Gao, Z.X., Cao, X.J., Qian, X.Q., Wang, W.M., 2012. Comparison of morphology parameters of blunt snout bream(*Megalobrama amblycephala* Yih) among Liangzi Lake,Poyang Lake and Yuni Lake. J. Huazhong Agric. Univ. 31 (01), 88–94.
Zhu, C.K., Pan, Z.J., 2022. Progress of karyotype studies on Siluriformes in China. Acta Hydrobiol. Sin. 46 (04), 657–673.